THE ANNALS OF "DUNAREA DE JOS" UNIVERSITY OF GALATI.
FASCICLE IX. METALLURGY AND MATERIALS SCIENCE
N^0. 3 – 2013, ISSN 1453 – 083X

CORROSION BEHAVIOR OF SOME MATERIALS IN 0.5 M AMMONIUM HYDROXIDE SOLUTION

Gina ISTRATE, Florentina POTECAŞU, Vasile BAŞLIU
"Dunărea de Jos" University of Galaţi, 111, Domnească Street, 800201, Galaţi, Romania
email: gina.nastase@ugal.ro

ABSTRACT

The present work has the purpose of studying metallographic aspects and corrosion resistance of three materials used in ammonia stripping plants. The corrosion process was evaluated by gravimetric tests and potentiodynamic method. Materials tested were Al 1050 (99.5%Al), stainless steel AISI 316Ti and low alloy steel P235TR2. To determine gravimetrically the rate of penetration, samples were immersed in corrosive environment for 294 days and weighed periodically. As test solution 0.5 M ammonium hydroxide (specific for coke industry) was used in a three electrode open cell with material tested as working electrode (WE), a platinum electrode as counter electrode (CE) and an Ag/AgCl electrode as reference electrode (RE).

KEYWORDS: corrosion, ammonium hydroxide, penetration index

1. Introduction

Corrosion process plays an important role in the field of economics and safety. Various types of materials are included in different industries (chemical and electrochemical industries, medical, nuclear, petroleum, power, and food production), and also in daily life.

In the stripping plants were used the following materials: aluminium Al 1050, stainless steel 316Ti and low alloy steel P235TR2.

The high affinity of aluminium for oxygen enables them to develop oxide films at room temperature and these films possess excellent adhesion, continuity and corrosion resistance properties. In atmospheres of low or moderate corrosivity, aluminium behaves as a passive material, but the insignificant corrosion that takes place is sufficient to deteriorate its appearance [1]. The corrosion behavior of commercial aluminium alloys was studied in many aqueous chemical environments [2-11]. Type 316Ti stainless steel has been widely used as sheet and tube materials in the chemical industry and nuclear power industry. Up to now, various environments have been investigated and reported for materials used in the circuit piping system and should be cautiously considered for purposes of safe operations and managements as well as remaining life assessment of different plants, among which corrosion is of great importance [12-16]. Corrosion behavior of low-alloy steel was investigated in many environments [17-24].

2. Experimental procedure

For weight loss measurements, the samples of materials (AISI Al 1050 (99.5%Al), stainless steel AISI 316Ti and low alloy steel P235TR2) were abraded with different emery papers (grade 800, 1000 and 1200), washed with double distilled water, rinsed with ethanol and acetone, and then dried at room temperature. After weighing accurately, the specimens were immersed in beakers containing 250mL of 0.5 M ammonium hydroxide solution, at 25^o C. After each immersion time, the specimens were taken out, washed, dried, and weighed accurately. In order to obtain good reproducibility, experiments were carried out in triplicate.

The corrosion rate (V_{corr}) and penetration index (P) were calculated from the following relations:

$$V_{corr} = \frac{\Delta m}{S \cdot t}[g \cdot m^{-2} \cdot h^{-1}] \quad (1)$$

where: Δm is the weight loss values, S is the total area in m^2 and t is the immersion time in h, and

$$P = \frac{24 \cdot 365 \cdot V_{corr}}{1000 \cdot \rho} \quad (2)$$

V_{corr}–corrosion rate, [g·m^{-2} ·h^{-1}]; ρ - density, [g·cm^{-3}].

Potentiodynamic polarization measurements were conducted using a VoltaLab-PGP-201.

A conventional cylindrical glass cell of 250mL with three electrodes was used. A platinum sheet of 2cm^2 area and Ag/AgCl electrode ($E_{Ag/AgCl}$=+200 mV/ENH) were used as auxiliary and reference electrodes, respectively.

The working electrode was embedded with epoxy except for the working surface.

Potentiodynamic polarization curves were obtained by varying the potential automatically from -300 to +300mV against the open circuit potential (OCP) with the scan rate of 2mVs^{-1} starting one hour after immersion of the working electrode into the test solution.

3. Results and discussion

In Figures 1-3 is shown the weight loss for the studied materials.

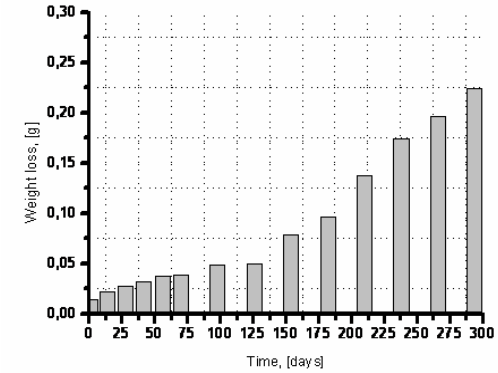

Fig. 1. *Weight loss vs. exposure time to corrosive environment NH_4OH 0.5M for Al 1050*

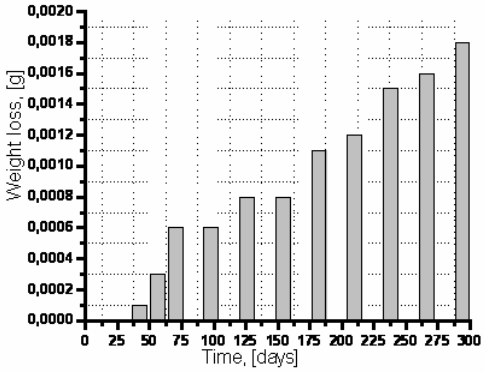

Fig. 2. *Weight loss vs. exposure time to corrosive environment NH_4OH 0.5M for 316Ti*

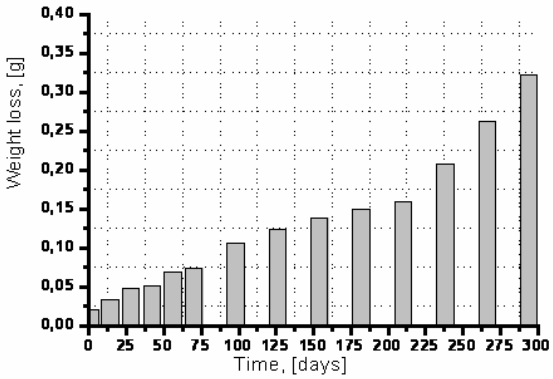

Fig. 3. *Weight loss vs. exposure time to corrosive environment NH_4OH 0.5M for P235TR2*

The values of the corrosion rate were obtained from weight loss measurements using Eqs. (1) at 25^{o}C and were listed in Table 1.

Table. 1*. Corrosion rate*

Sample	**Al 1050**	**316Ti**	**P235TR2**
Time [days]	**Corrosion rate** $V_{cor} = \Delta m/(S \cdot t)$ [g/m^2·h]		
1	$356.167 \cdot 10^{-3}$	0	$555.555 \cdot 10^{-3}$
14	$39.032 \cdot 10^{-3}$	0	$64.682 \cdot 10^{-3}$
28	$24.307 \cdot 10^{-3}$	0	$46.626 \cdot 10^{-3}$
42	$18.528 \cdot 10^{-3}$	$196 \cdot 10^{-6}$	$33.664 \cdot 10^{-3}$
56	$16.205 \cdot 10^{-3}$	$442 \cdot 10^{-6}$	$33.928 \cdot 10^{-3}$
70	$13.452 \cdot 10^{-3}$	$708 \cdot 10^{-6}$	$29.166 \cdot 10^{-3}$
98	$12.247 \cdot 10^{-3}$	$506 \cdot 10^{-6}$	$29.875 \cdot 10^{-3}$
126	$9.680 \cdot 10^{-3}$	$524 \cdot 10^{-6}$	$27.226 \cdot 10^{-3}$
154	$12.403 \cdot 10^{-3}$	$429 \cdot 10^{-6}$	$24.855 \cdot 10^{-3}$
182	$12.867 \cdot 10^{-3}$	$499 \cdot 10^{-6}$	$22.741 \cdot 10^{-3}$
210	$15.949 \cdot 10^{-3}$	$472 \cdot 10^{-6}$	$21.137 \cdot 10^{-3}$
238	$17.845 \cdot 10^{-3}$	$521 \cdot 10^{-6}$	$24.159 \cdot 10^{-3}$
266	$18.066 \cdot 10^{-3}$	$497 \cdot 10^{-6}$	$27.474 \cdot 10^{-3}$
294	$18.603 \cdot 10^{-3}$	$506 \cdot 10^{-6}$	$30.432 \cdot 10^{-3}$

From the graph shown in Figure 4 it have be seen that samples Al 1050 - 1 day of immersion has a high penetration index of 1155 mm/year thereafter greatly decreases averaging $50 \bullet 10^{-3}$mm/year.

In Figures 4-6 are shown the values of penetration index for the studied materials, calculated with relation 2.

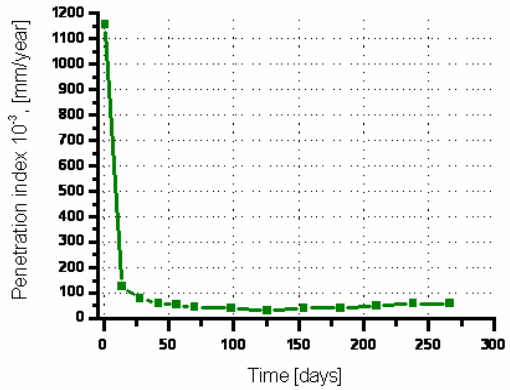

***Fig. 4.** Penetration index vs. time for Al 1050*

This shows that the sample surface was covered with a layer of aluminum oxide which greatly reduces the corrosion rate.

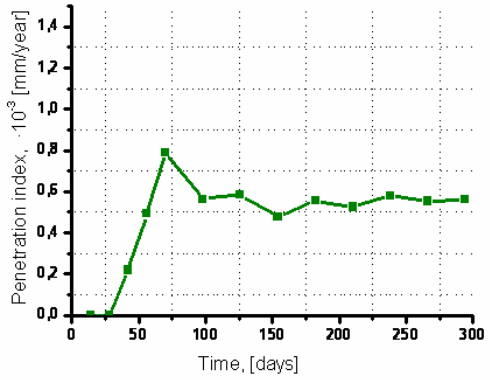

***Fig. 5.** Penetration index vs. time for 316Ti*

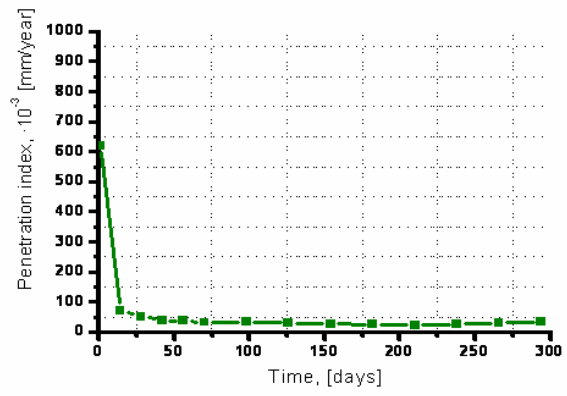

***Fig. 6.** Penetration index vs. time for P235TR2*

From the graph shown in Figure 5 we can see that samples from 316Ti present the first weighing, zero mass loss, only at 42 – day, they show a weight loss of $1 \bullet 10^{-4}$g, and until the end of the analysis the average penetration index of $500 \bullet 10^{-6}$ mm/year.

Corrosion of gravity detected in 0.5M NH_4OH was evidenced by metallographic analysis on the surface of the sample subject to corrosion during a period of 294 days. In Figures 7-9 are shown some microstructures of the materials studied, before and after immersion in 0.5M NH_4OH for 294 days. The changes induced by different mechanisms from corrosion, at the interface of Al 1050/ corrosive environment were studied in comparison to control samples of Al 1050 (before the corrosion).

In Figure 7.a. there is a bright appearance of the original sample surface with a less specific roughness and small imperfections (scratches, nicks).

After the immersion period of 294 days, the surface morphology is deeply modified (Figs. 7.b. and 7.c.). Passivated surface is degraded initially, strong and bright appearance disappeared, being replaced by darker large areas. It appears that the mechanisms of degradation of the material due to corrosion are complex, so it appears that in addition to continuous corrosion (the entire metal surface has suffered from aggressive environmental action) shows a local corrosion (due to structural imperfections, nonmetallic inclusions, internal microtensions by second order) as evidenced by:

- corrosion spots - large portions and relatively small depth;
- corrosion plate - relatively small areas but greater depths;
- points of corrosion (Pitting) - concentrated on small and deep areas (with diameters up to 100 μm).

316Ti stainless steel samples (Fig.8.) show a very high chemical stability. The area has not changed significantly (probably light intercrystalline corrosion phenomena limit small chemical compounds precipitated in the metallic matrix). Microstructures for P235TR2 show the generalized deep corrosion in spots and points of corrosion (pitting). In Fig. 9.a on the polished sample and whitout metallographic attack it can be seen a steel with small quantity of nonmetallic inclusions (score 1.5-2). The macro-metallographic analysis reveals that in the presence of heterogeneous structures (pearlite) the corrosion process is intensified because grain dispersed phases are in contact and the alloy behaves like two metals which are in contact in the same corrosive environment (fig. 9.b.). The presence of non-metallic inclusions favors accelerated local corrosion. The typical anodic potentiodynamic polarization curves of material tested, measured in NH_4OH 0.5 M solutions, are shown in Fig. 9.

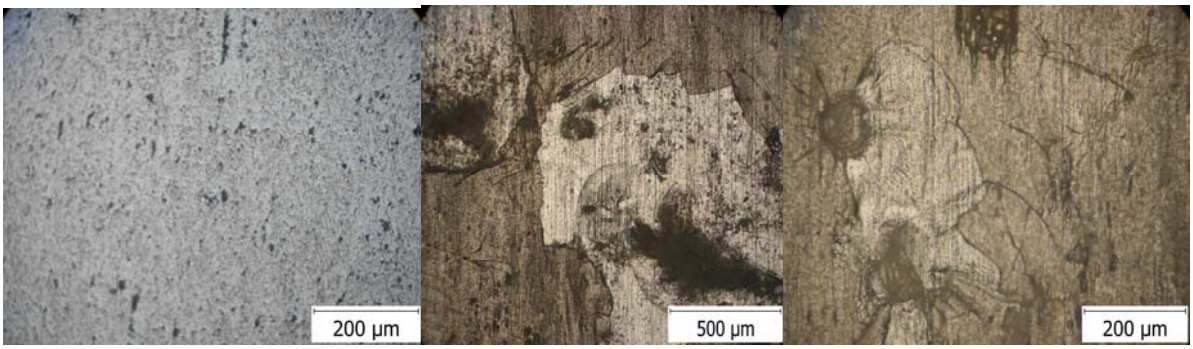

a) b) c)

Fig. 7. *The metallographic aspect of Al 1050 samples before (a) and after immersion for 294 days in NH_4OH 0.5 M*

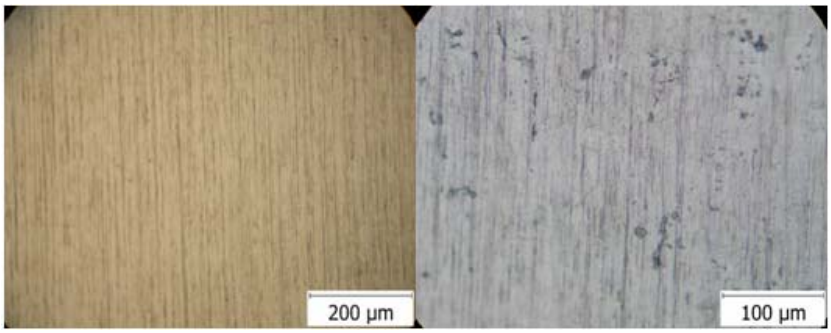

Fig. 8. *The metallographic aspect of 316Ti samples before and after immersion For 294 days in NH_4OH 0.5 M*

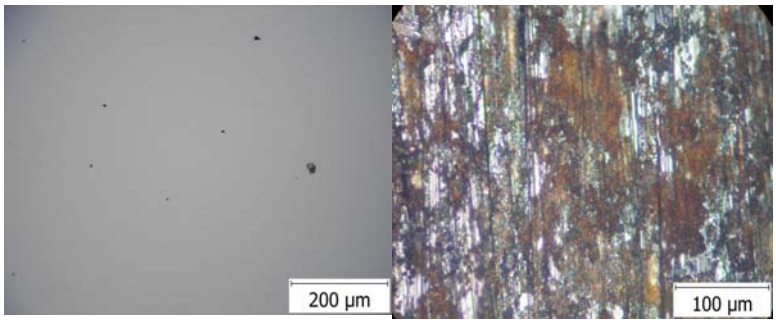

Fig. 9. *The metallographic aspect of P235TR2 samples before and after immersion For 294 days in NH_4OH 0.5 M*

Corrosion rates of the coatings were derived from the Stern–Geary equation:

$$i_{corr} = \frac{1}{2.303 R_p}\left(\frac{\beta_a \cdot \beta_c}{\beta_a + \beta_c}\right) \qquad (3)$$

- i_{corr} is the corrosion current density in Amps/cm^2;
- R_p is the corrosion resistance in ohms cm^2;
- β_a is the anodic Tafel slope in Volts/decade or mV/decade of current density;
- β_c is the cathodic Tafel slope in Volts/decade or mV/decade of current density;
- the quantity, $(\beta_a \cdot \beta_c)/(\beta_a + \beta_c)$, is referred to as the Tafel constant.

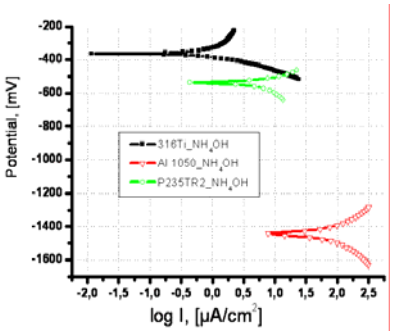

Fig. 9. *Comparative polarization potentiodynamic curves for tested materials in 0.5M NH_4OH solution obtained after 60 minutes of immersion time*

The polarization resistance, Rp, was determined from the slopes of the potential-current plots measured by the linear polarization curve (LSV) at a scanning rate of 2 mV/s.

The corrosion potential (E_{corr}), corrosion current density (i_{corr}) and polarisation resistance (R_p), which were obtained from the potentiodynamic polarisation curves are summarized in Table 2.

From potentiodynamic polarization curves the polarization resistance for Al 1050 was 0.74 kΩ·cm^2. For 316Ti stainless steel samples the polarization resistance was 29.26 kΩ·cm^2.

Table 2. *Results from the potentiodynamic polarisation curves for the tested materials*

No.	Tested material	Ecor, mV Ag/AgCl	βa	βc	icor	Rp	Vcor
			[mV/dec]		[μA/cm²]	[kΩ·cm^2]	[μm/an]
1.	Al 1050	-1443.5	322.3	380.0	102.32	0.74	1115
2.	316Ti	-360.0	478.0	125.0	1.47	29.26	17.21
3.	P235TR2	-585.4	311.1	409.9	8.90	8.62	103.14

4. Conclusions

The results obtained from weight loss and electrochemical studies were in reasonable agreement for low alloy steel P235TR2. Microstructures for P235TR2 present profound generalized corrosion, spots and points of corrosion (pitting).

The samples of 316Ti stainless steel show a very high chemical stability.

After the immersion of 294 days, the surface morphology of Al 1050 is profoundly altered. Passivated surface is degraded, strong and bright appearance initially disappeared, being replaced by darker large areas.

From the electrochemical results, it can be seen that the corrosion potential of Al 1050 tends to more negative values, hence it is deducted that the polarization resistance value is the smallest (of the order of Ω) in comparison to other materials whose polarization resistance is of the order kΩ. The corrosion rate calculated has the highest value for Al 1050 (1.115mm/year) and the lowest for 316Ti (17.21μm/year).

References

[1]. M.J. Bartolomé, J.F. del Río, E. Escudero, S. Feliu Jr., V. López, E. Otero, J.A. González - *Behaviour of different bare and anodised aluminium alloys in the atmosphere*, Surface & Coatings Technology 202 (2008) 2783–2793.

[2]. Monica Trueba, Stefano P. Trasatti - *Study of Al alloy corrosion in neutral NaCl by the pitting scan technique,* Materials Chemistry and Physics 121, 2010, 523-533.

[3]. A. García-Romero, A. Delgado, A. Urresti, K. Martín, J.M. Sala - *Corrosion behaviour of several aluminium alloys in contact with a thermal storage phase change material based on Glauber's salt,* Corrosion Science 51 (2009) 1263–1272.

[4]. Serpil Şafak, Berrin Duran, Aysel Yurt, Gülşen Türkoğlu - *Schiff bases as corrosion inhibitor for aluminium in HCl solution*, Corrosion Science, Volume 54, January 2012, Pages 251–259.

[5]. Zhenhua Dan, Izumi Muto, Nobuyoshi Hara, *Effects of environmental factors on atmospheric corrosion of aluminium and its alloys under constant dew point conditions*, Corrosion Science, Volume 57, April 2012, Pages 22–29.

[6]. S.M. Abd El Haleem, S. Abd El Wanees, E.E. Abd El Aal, A. Farouk - *Factors affecting the corrosion behaviour of aluminium in acid solutions. I. Nitrogen and/or sulphur-containing organic compounds as corrosion inhibitors for Al in HCl solutions*, Corrosion Science, Volume 68, March 2013, Pages 1–13.

[7]. E.E. Abd El Aal, S. Abd El Wanees, A. Farouk, S.M. Abd El Haleem - *Factors affecting the corrosion behaviour of aluminium in acid solutions. II. Inorganic additives as corrosion inhibitors for Al in HCl solutions*, Corrosion Science, Volume 68, March 2013, Pages 14–24.

[8]. X. Zhou, C. Luo, T. Hashimoto, A.E. Hughes, G.E. Thompson - *Study of localized corrosion in AA2024 aluminium alloy using electron tomography*, Corrosion Science, Volume 58, May 2012, Pages 299–306.

[9]. R. Arrabal, B. Mingo, A. Pardo, M. Mohedano, E. Matykina, I. Rodríguez - *Pitting corrosion of rheocast A356 aluminium alloy in 3.5wt.% NaCl solution*, Corrosion Science, Volume 73, August 2013, Pages 342–355.

[10]. N. Murer, R.G. Buchheit - *Stochastic modeling of pitting corrosion in aluminum alloys*, Corrosion Science, Volume 69, April 2013, Pages 139–148.

[11]. WANG Zhen-yao, MATeng, HAN Wei, W Guo-cai - *Corrosion behavior on aluminum alloy LY 12 in simulated atmospheric corrosion process,* Trans. Nonferrous Met**.** SOC. China l7 (2007) 326-333.

[12]. A. Pardo, M.C. Merino, A.E. Coy, F. Viejo, R. Arrabal, E. Matykina - *Pitting corrosion behaviour of austenitic stainless steels – combining effects of Mn and Mo additions*, Corrosion Science 50 (2008) 1796–1806.

[13]. J. M.A. Van der Horst - *Corrosion of stainless steel by aqua ammonia*, Corrosion Science, 1972, Vol. 12, pp. 761 to 765. Pergamon Press, Printed in Great Britain.

[14]. A. Pardo, M.C. Merino, M. Carboneras, F. Viejo, R. Arrabal, J. Muñoz - *Influence of Cu and Sn content in the corrosion of AISI 304 and 316 stainless steels in H_2SO_4,* Corrosion Science 48 (2006) 1075–1092.

[15]. A. Pardo, M.C. Merino, A.E. Coy, F. Viejo, M. Carboneras, R. Arrabal - *Influence of Ti, C and N concentration on the intergranular corrosion behaviour of AISI 316Ti and 321 stainless steel*, Acta Materialia 55 (2007) 2239–2251.

[16]. A. Pardo, M.C. Merino, A.E. Coy, F. Viejo, R. Arrabal, E. Matykina - Effect of Mo and Mn additions on the corrosion behaviour of AISI 304 and 316 stainless steels in H2SO4, Corrosion Science 50 (2008) 780–794.

[17]. J.H. Hong, S.H. Lee, J.G. Kim, J.B. Yoon - *Corrosion behaviour of copper containing low alloy steels in sulphuric acid*, Corrosion Science, Volume 54, January 2012, Pages 174–182.

[18]. Keon Ha Kim, Seung Hwan Lee, Nguyen Dang Nam, Jung Gu Kim - *Effect of cobalt on the corrosion resistance of low alloy steel in sulfuric acid solution*, Corrosion Science, Volume 53, Issue 11, November 2011, Pages 3576–3587.

[19]. Lining Xu, Shaoqiang Guo, Wei Chang, Taihui Chen, Lihua Hu, Minxu Lu - *Corrosion of Cr bearing low alloy pipeline steel in CO_2 environment at static and flowing conditions*, Applied Surface Science, Volume 270, 1 April 2013, Pages 395–404.

[20]. Mohammed A. Amin, Gaber A.M. Mersal, Q. Mohsen - *Monitoring corrosion and corrosion control of low alloy ASTM A213 grade T22 boiler steel in HCl solutions*, Arabian Journal of Chemistry, Volume 4, Issue 2, April 2011, Pages 223–229

[21]. J.B. Sun, G.A. Zhang, W. Liu, M.X. Lu - *The formation mechanism of corrosion scale and electrochemical characteristic of low alloy steel in carbon dioxide-saturated solution*, Corrosion Science, Volume 57, April 2012, Pages 131–138.

[22]. Nabel A. Negm, Nadia G. Kandile, Emad A. Badr, Mohammed A. Mohammed - *Gravimetric and electrochemical evaluation of environmentally friendly nonionic corrosion inhibitors for carbon steel in 1 M HCl*, Corrosion Science, Volume 65, December 2012, Pages 94–103.

[23]. A. Contreras, S.L. Hernández, R. Orozco-Cruz, R. Galvan-Martínez - *Mechanical and environmental effects on stress corrosion cracking of low carbon pipeline steel in a soil solution*, Materials & Design, Volume 35, March 2012, Pages 281–289.

[24]. Octavian Potecaşu, Florentina Potecaşu, Marian Bordei, Petrică Alexandru, Florin Marin - *The corrosion behavior of steel for transportation of petroleum products in marine environment*, International Multidisciplinary Scientific GeoConference, SGEM2013, Conference Proceedings, ISBN 978-954-91818-8-3 / ISSN 1314-2704, June 16-22, 2013, Vol. 2, 981 - 988 pp.